SCIENTIFIC REPORTS

OPEN

SUBJECT AREAS:
ELECTRONIC DEVICES
POLYMER SYNTHESIS

Received
8 May 2014

Accepted
11 June 2014

Published
27 June 2014

Correspondence and requests for materials should be addressed to H.J.S. (hjson@kist.re.kr) or D.S.C. (dchung@cau.ac.kr)

High mobility polymer based on a π-extended benzodithiophene and its application for fast switching transistor and high gain photoconductor

Sungmin Park[1,3], Byung Tack Lim[2], BongSoo Kim[1], Hae Jung Son[1] & Dae Sung Chung[2]

[1]Photo-electronic Hybrids Research Center, Korea Institute of Science and Technology (KIST), Seoul, 136-791, Republic of Korea, [2]School of Chemical Engineering and Material Science, Chung-Ang University, Seoul, 156–756, Korea, [3]Department of Chemistry, Korea University, Seoul 136-713, Republic of Korea.

Here we present synthesis and electronic properties of a new alternating copolymer composed of dithieno[2,3-*d*;2′,3′-*d*′]benzo[1,2-*b*;4,5-*b*′]dithiophene (DTBDT) and diketopyrrolopyrrole units, poly dithienobenzodithiophene-co-diketopyrrolopyrrolebithiophene (PDPDBD). The resulting polymer showed hysteresis free, fast switching and highly reliable organic thin-film transistor properties comparable to a-Si. Hole mobility of the polymer is about 2.7 $cm^2V^{-1}s^{-1}$, which is remarkably improved compared with its benzodithiophene (BDT)-analougue that contains a smaller aromatic ring of BDT in the place of DTBDT. This is mainly due to much increased intramolecular charge transport originated from PDPDBD's rigid molecular backbone. Furthermore, photoconductor devices fabricated by using PDPDBD as an active layer showed a high performance with the highest photoconductive gain of ~10^5. Taken together, the successful PDPDBD's transistor and photoconductor performances with high device stability demonstrated practical applicability of PDPDBD in low-cost and flexible optoelectronic devices.

Conjugated polymer-based organic field effect transistors (OFETs) have attracted much attention as electronic switching elements in futuristic flexible electronics because they can be fabricated using solution processes on plastic substrates at low costs[1–5]. Compared with conventional inorganic semiconductors, the synthetic versatility of conjugated polymers allows the discovery of various new materials with controlled structures and physical properties[6–9]. Over the last decade, the synergistic development of new conjugated polymers and device fabrication technologies has resulted in a few conjugated polymer-based OFETs having very high charge carrier mobilities (>1 $cm^2\ V^{-1}s^{-1}$), exceeding those of amorphous silicons[10–16]. However, in spite of such remarkable development in the area of conjugated polymers, key challenges still remain for commercial viability: it is required that OFETs achieve high charge carrier mobilities and maintain initial device performance characteristics while operating under ambient conditions. For this, it is highly important to develop stable high charge carrier mobility conjugated polymers[10,17–20]. One of the most effective ways to increase the charge carrier mobility is to incorporate a fused aromatic ring with an extended π-conjugation into the polymer backbone. This promotes enhanced intermolecular π-π interactions of the conjugated polymer by reducing conformational backbone disorder and increasing molecular rigidity of the polymer in the solid state, which facilitates intra- and intermolecular charge transport in the polymer[21–24]. Incorporating fused heteroaromatic compounds such as heteroacenes into the polymer backbone is a particularly good approach to improve polymer stability and chare carrier mobility. Compared with benzene-based acenes (e.g. pentacene) whose low stability in air imparts detrimental effects on FET mobility under ambient conditions, the heteroacenes can effectively improve the air stability of the polymer by lowering the HOMO energy level of the polymer[25,26]. Furthermore, heteroatoms in the heteroaromatic compounds promote increased intermolecular interactions by inducing various non-covalent interactions such as sulfur-sulfur and sulfur-oxygen interactions, leading to enhanced charge carrier mobility of the polymer[25,27,28].

In our research, as a building block for conjugated polymers with a high charge carrier mobility, we chose dithieno[2,3-*d*;2′,3′-*d*′]benzo[1,2-*b*;4,5-*b*′]dithiophene (DTBDT). This monomer unit was designed by annulating two thiophene rings at the terminals of benzo[1,2-*b*;3,4-*b*′]dithiophene (BDT), which is a good building block for high-performance organic semiconductors with high air stabilities[29–33]. A push-pull type copolymer based on

DTBDT was prepared by employing a diketopyrrolopyrrole (DPP) moiety as an electron acceptor unit, which helps to increase the intermolecular interactions between the polymer chains due to its remarkable aggregation properties, and thereby to improve the charge carrier mobility. In addition, the electron-deficient DPP is expected to contribute to increase of the air stability of the polymer[8,34,35].

Herein, we present synthesis and OFET properties of a new alternating copolymer composed of DTBDT and DPP units, poly dithienobenzodithiophene-co-diketopyrrolopyrrolebithiophene (PDPDBD) (Figure 1). The resulting polymer showed a high hole mobility of 2.7 $cm^2V^{-1}s^{-1}$, which is a remarkable improvement from 0.005 $cm^2V^{-1}s^{-1}$ for benzodithiophene-co-diketopyrrolopyrrolebithiophene (PDPBD) incorporating a smaller aromatic ring of BDT in the place of DTBDT. It is discussed that DTBDT in the polymer plays an important role for improving intramolecular charge transport by increasing rigidity of the polymer backbone. Notably, the prepared polymer PDPDBD exhibited high stability while operating under ambient conditions. Due to the high charge carrier mobility of PDPDBD, PDPDBD -based low voltage transistors showed fast switching behaviors with an operation frequency up to ~20 KHz and photoconductor devices using PDPDBD as an active layer demonstrated the highest photoconductive gain of $\sim 10^5$.

Experimental procedures. *Synthesis of* PDPDBD: 3,6-bis(5-bromothiophene-2-yl)- *N*, *N* ′-bis(2-decyltetradecyl)-1,4-dioxopyrrolo[3,4-*c*]pyrrole (147.1 mg, 0.13 mmol) was weighed into a 10 mL round-bottom flask. Then, 5,10-bis(2-hexyldecyl)dithieno[2,3-*d*:2′,3′-*d*′]benzo[1,2-*b*:4,5-*b*′]dithiophene-2,7-diyl)bis(trimethylstannane) (110.8 mg, 0.13 mmol) and tetrakis(triphenylphosphine)palladium(0) ($Pd(PPh_3)_4$) (6.5 mg) were added. The flask was subjected to five successive cycles of vacuum followed by refilling with argon. Anhydrous dimethylformamide (DMF) (0.5 mL) and anhydrous toluene (2.0 mL) were added via a syringe. The Stille coupling polymercondensation readtion was carried out at 120° C for 36 h under argon protection. The resulting product was precipitated into methanol and collected by filtration. The catalyst impurities and oligomers were removed by Soxhlet extraction with hexane, methanol, and chloroform. The resulting solid from the chloroform fraction was obtained after drying in vacuo overnight (157.4 mg, 80.9%). ^{1}H NMR (400 MHz, $CDCl_2CDCl_2$) δ 0.68–1.77 (b, 124H), 2.82–4.59 (b, 8H), 6.45–7.78 (b, 4H), 8.32–9.79 (b, 2H). GPC: M_n = 28.9 kg/mol; PDI = 2.60.

Device fabrication: Top-contact OFETs were fabricated on a common gate of highly n-doped silicon with a 300 nm thick thermally grown SiO_2 dielectric layer. Thin layer of Cytop™ was spin-coated onto SiO_2 dielectric layer (~20 nm). For sol-gel processed ZrOx layer to fabricate low voltage device, a zirconium(IV) acetylacetonate ($Zr(acac)_4$) solution in N, N -dimethylformamide(DMF) was spin-coated on a heavily doped Si wafer and cured under high temperature (400°C) for 1 hour.

Capacitance of such dielectric layer was measured using an SR 720 LCR meter at frequencies ranging from 100 Hz to 100 kHz. (MIM device structure was used.) The capacitance value measured at 100–120 Hz and 9.1 nF/cm^2 was used to extract the charge carrier mobility in the case of SiO_2 device and 320 nF/cm^2 in the case of low voltage device. Solutions containing the polymer semiconductors were spin-coated at 2000 rpm from 0.2 wt% chloroform solutions to form thin films with a nominal thickness of 40 nm, as confirmed using a surface profiler (Alpha Step 500, Tencor). The films were annealed at 200°C for 10 min under a nitrogen atmosphere. Gold source and drain electrodes were evaporated on top of the semiconductor layers (60 nm). For all measurements, typical channel widths (*W*) and lengths (*L*) were 1000 μm and 50 μm, respectively.

Device characterization: Electrical characteristics of fabricated devices were measured in air using both Keithley 236 and Keithley 2400 source/measure units combined with home-built Labview program. Gate bias signals with various frequencies were provided by arbitrary function generator (AFG310, Tektronix) and the source-drain responses were recorded using either Labview program or Digital Phosphor Oscilloscope (TDS 5052, Tektronix) depending on the time scale. Temperature dependence of transistor performances were recorded using a vacuum cryogenic chamber connected to the other required electronics. An atomic force microscope (AFM, Multimode SPM, Digital Instruments) was used to characterize the surface morphologies of polymers. GIXS studies were performed at the 3C beamline at the Pohang Accelerator Laboratory (PAL). The measurements were carried out with a sample-to-detector distance of 214.111 mm. Data were typically collected for thirty seconds using an Xray radiation source of 1.1785 nm with a 2D charge-coupled detector (CCD) (Roper Scientific, Trenton, NJ, USA) The incidence angle for the X-ray beam was set to 0.17°, which was intermediate between the critical angles of the films and the substrate. In the case of photoconductor measurement, the current density–voltage (*J*–*V*) characteristics and transient photocurrent were measured using Keithley 2400 source/measure units under the monochromatic light from a 150 W Xenon arc lamp assembled with a 1/8 m monochromator operating by home-built Lab-view program. To test a shelf-life characteristics of the device, transfer curve was first measured directly after fabrication and then after several days of storage under ambient oxygen and under ambient humidity conditions (30–40%) in the dark. The operating stress stability was measured under the same condition.

Results and discussion

PDPDBD was synthesized via the Stille polycondensation reaction of a ditin compound of DTBDT and a DPP dibromide, as shown in Figure 1. The resulting polymer was precipitated in methanol and catalyst impurities and oligomers were subsequently removed by Soxhlet extraction. PDPDBD showed good solubility in chlorinated solvents such as chloroform, chlorobenzene, and 1, 2-dichlorobenzene. The molecular weight (M_n) of the polymer is 28.9 kg/mol with a polydispersity index (PDI) of 2.60. Thermogravimetric analysis (TGA) indicates that the polymer is stable up to about 400°C. (Supplementary Information, Figure S2). For the both polymers, no clear glass transition was observed from 30 to 270°C in the differential scanning calorimetry (DSC) curves of the second heating and cooling runs (5°C/min) (SI, Figure S3). The absorption spectra of PDPDBD in chloroform solution and as a thin film are shown in Figure 2. The maximum peak (λ_{max}) and the onset point (λ_{onset}) in the spectra were red-shifted from the solution phase (λ_{max}= 752 nm, λ_{onset}= 791 nm) to the film (λ_{max}= 759 nm, λ_{onset}= 814 nm), indicating that the polymer backbone becomes more planar and that the

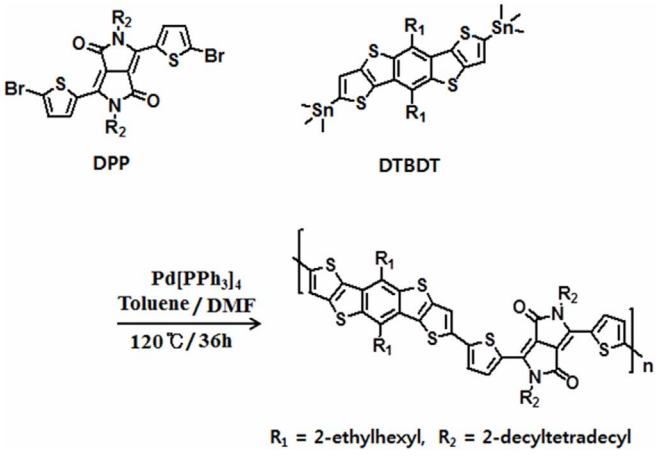

Figure 1 | **Synthetic route for PDPDBD.**

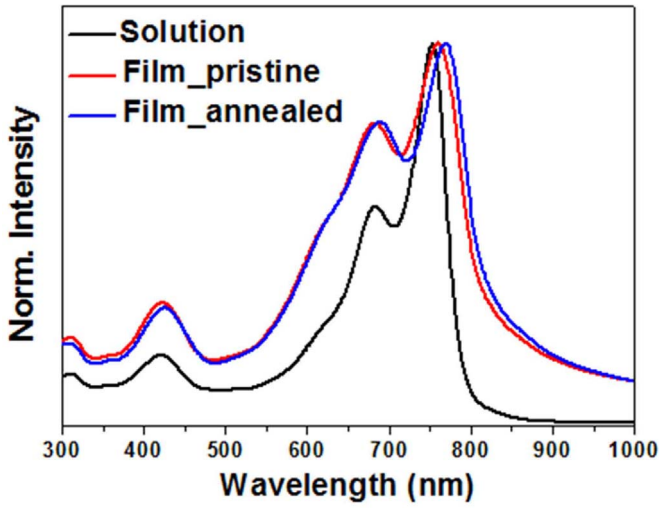

Figure 2 | UV-Vis absorption spectra of the dilute chloroform solution and thin film with/without thermal annealing of PDPDBD.

π-electrons are more delocalized along the polymer chain due to increased intermolecular interactions in the film. Thermal annealing of the polymer thin film at 200°C resulted in a slight red-shift in the absorption peaks, which suggests that annealing induced higher ordering of the polymer structures. The optical energy bandgap (E_g) of PDPDBD was estimated to be ~1.52 eV from λ_{onset} in the spectrum of the film. By cyclic voltammetry, the highest occupied molecular orbital (HOMO) level and the lowest unoccupied molecular orbital (LUMO) were measured to be −5.39 eV and −3.38 eV, respectively. Note that the HOMO level is quite lower compared with other DPP-based polymers, from which one can expect lower susceptibility of PDPDBD against air oxidation[8].

Figure 3 shows the output and transfer characteristics of OFETs employing PDPDBD thin films as a semiconductor layer which were prepared with and without thermal annealing at 200°C. It is notable that the OFET prepared without thermal annealing achieved a high hole mobility of 1.4 $cm^2\ V^{-1}s^{-1}$ and an on/off ratio of ~10^7. In our experiments, more than ten devices among seventy tested devices showed hole mobilities over 1 $cm^2\ V^{-1}\ s^{-1}$ without any post treatment. Such annealing free high mobilty phenomenon is often observed in donor-acceptor type polymers particularly when the polymer repeating unit include strong acceptors[36–38]. This result implies that PDPDBD can form favorable charge transport pathways even at a room temperature. Importantly, the transfer characteristics in the saturation regime showed negligible hysteresis between off-to-on and on-to-off sweeps. The OFET performance was further improved by thermal annealing of the thin films and the best results were observed when annealed at 200°C. The resulting device exhibited a much higher hole mobility of 2.7 $cm^2V^{-1}s^{-1}$, and a smaller hysteresis than devices without thermal anealing. The device hysteresis, defined as the difference between the threshold voltages measured during off-to-on and on-to-off sweeps, was 3.2 V and 2.5 V for pristine and annealed devices, respectively. Considering the large voltage sweep window of 120 V, the measured hysteresis is very small in comparison with other reported OFETs[39–41]. To further study how the OFET performance is affected by the incorporation of DTBDT into the conjugated polymers, we prepared a BDT-analogue polymer of PDPBD, where the DTBDT unit was replaced by a smaller heteroacene BDT. It has been reported that alternating copolymers consisting of BDT and DPP showed low OFET mobilities in the range of $10^{-4} \sim 10^{-3}$ $cm^2V^{-1}s^{-1}$ [42]. In our OFET measurement (SI, Figure S5), PDPBD showed a hole mobility at most of 0.005 $cm^2\ V^{-1}s^{-1}$ under the same device fabrication conditions as that of PDPDBD, which is slightly better than the reported value, but still much lower than that

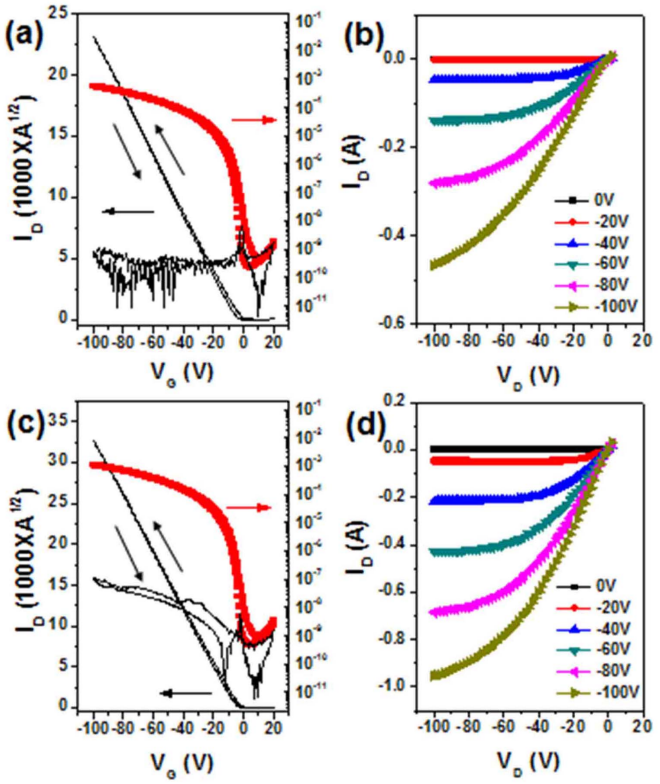

Figure 3 | Representative transfer and output curves of OFETs from PDPDBD without thermal annealing (a,b) and with thermal annealing (c,d).

of PDPDBD. Overall, these OFET results suggest that incorporation of DTBDT with an extended π-conjugation into the pull-push type polymer is a successful synthetic strategy for enhancing charge carrier transport.

In order to investigate the charge transport properties in more detail, we study the temperature dependence of transfer characteristics. In a plot of $I_{DS}^{1/2}$ vs V_{GS} measured by off-to-on sweep direction (Figure 4(a)), the mobility of the device was increased as a function of the measurement temperature. The positive temperature coefficient of the mobility clearly indicates that the hopping transport mechanism is valid in PDPDBD, which is consistent with other high mobility polymer semiconductors[10]. The obtained mobilities were plotted as a functon of inverse temperature in Figure 4(b), and the result demonstates that the temperature dependence of the mobility follows Arrhenius behavior. The Arrhenius activation energy was estimated to be ~40 meV, which is among the lowest values reported for high performance conjugated polymers[10,43–45]. The V_{th} shift was also monitored as a function of temperature and is summarized in Fig. 4(c). We can approximately estimate the concentration of deep trap states from the equation[46]: $N_{tr} = \frac{C_i V_{th}}{e}$, to be ~$4.2 \times 10^{10}$ cm^{-2} at room temperature. As temperature decreases, the density of deep trap states increases up to ~2×10^{11} cm^{-2} at 185K. Considering that, in the hopping transport model, the charge carrier hopping rate betwen sites *i* and *j* can be expressed by $v_{ij} \sim exp\left(-\frac{E_j - E_i}{kT}\right)$[47], we can say that the result – increasing trap densities at low temperature – also strongly supports hopping transport in this polymer. Furthermore, the logarithmic temperature dependence of V_{th} (Figure 3(c)) and the relation $\frac{\partial N_{tr}}{\delta E} \sim \frac{\partial V}{\partial T}$[46] suggest that the trap distribution in PDPDBD above its HOMO level follows an exponential distribution, which is similar to that of a-Si[48]. The trap distribution in

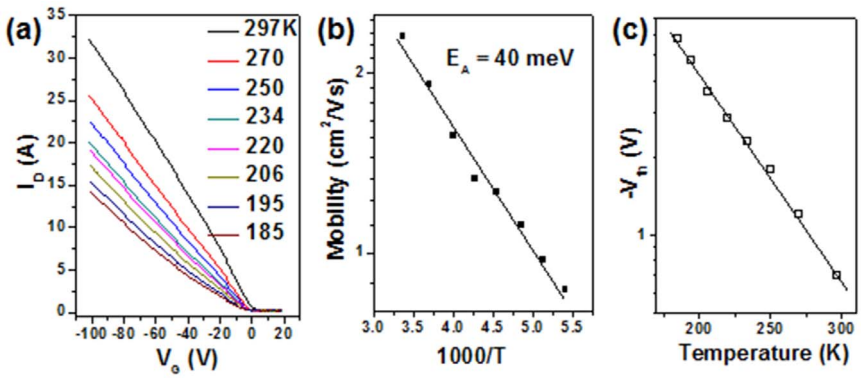

Figure 4 | (a) Temperature dependences of transfer characteristics (b) charge carrier mobility against inverse of temperature and (c) V_{th} against temperature.

this OTFT can be mainly attributed to the polymer bulk because we used hydroxy-free Cytop as the dielectric interface. When consider this result and the small activation energy of 40 meV, it is concluded that the high charge carrier mobility is explained by the low density of deep trap states in the polymer.

Although the mobility of the PDPDBD-based OFETs far exceeds that of a-Si, the electrical stability of the device is another critical issue that OFETs must satisfy for practical usages. OFETs often experience transfer curve shifts and thus ΔV_{th} due to unintended trapping of charge carriers. Such trapping of the charge carriers occurs in defect sites of the bulk polymer semiconductors, dielectrics, and interfaces of the two layers, which are formed when the device is exposed to electrical stress or ambient conditions for a long time. Therefore, to investigate the stability of the PDPDBD-bsed OFETs, the devices fabricated using optimal conditions were subjected to air/electrical stress and their charge transfer characteristics were systematically analyzed. Figure 5(a) shows the results of the shelf-lifetime tested over seven weeks. During the test, the devices were kept in ambient conditions without insulating the device from exposure to atmospheric air/moisture and lab-light. From the test of three devices, no appreciable changes in mobility and on/off ratio were observed, revealing excellent air-stability of the device. Because electrical stability of the OFET is also important, the effect of electrical stress on the device was investigated. Under a continuous supply of gate voltage at −100 V and drain voltage at −100 V, the transfer characteristics of the OFET were measured every 500 sec and plotted up to 50000 sec, as shown in Figure 5(b). Negative shifts of the transfer characteristics were observed because of hole trapping at electrical-stress induced-defects in the semiconductor/dielectric interfaces. However it is worthwhile to note that the ΔV_{th} is only ~2.5 V during 50000 sec of stress.

For quantatitive analysis of the electrical instability of PDPDBD-based OFETs, the ΔV_{th} was determined from the $I_{DS}^{1/2}$ vs V_G curve, as a function of exposure time to electrical stress, and is summarized in Figure 5(c). For an exponential distribution of deep trap states, as verified in the previous session for PDPDBD, a stretched-exponential decay model of ΔV_{th} with time can be used as follows[48]:

$$\Delta V_{th}(t) = (V_G - V_{th,0})\left[1 - exp\left\{-\left(t/\tau\right)^{\beta}\right\}\right] \quad (1)$$

where $V_{th,0}$ is the threshold voltage at the start of the experiment, τ is a characteristic time, and β is the dispersion parameter. Using this equation, we can fit the experimentally obtained plot of ΔV_{th} versus time and quantify the bias-stress stability of PDPDBD based OFETs. As shown in Figure 4(c), excellent agreement is obtained between the experimetal plot and theoretical fittng with a characteristic time τ of 6.9 × 10^7 sec. The observed characteristic time at room temperature is comparable to the highest value reported for a-Si transistors (8 × 10^7 sec), and is much higher than that of small-molecular semiconductor-based transistors and other polymer transistors[48,49]. Furthermore, the uniformity of PDPDBD -based OFETs was tested using 100 devices fabricated under the same condition and the distribtution of V_{th} was summarized in the Figure S6 of the Supplementary Information. Among 100 OFETs, the minimum and the maximun V_{th} was −3.25 and 2.4 V, respectively, with the average value of −0.51 V and the standard deviation of 1.3 V, implying excellent reproducibiliy of PDPDBD-based OFETs.

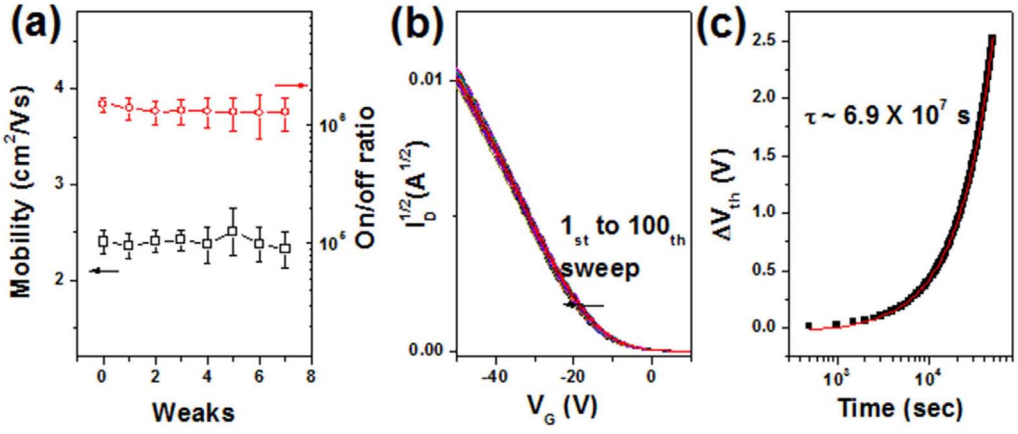

Figure 5 | (a) The results showing shelf life stability under ambient condition for charge carrier mobility and on/off ratio (b) Transfer characteristics and (c) ΔV_{th} measured during prolonged bias stress under ambient condition.

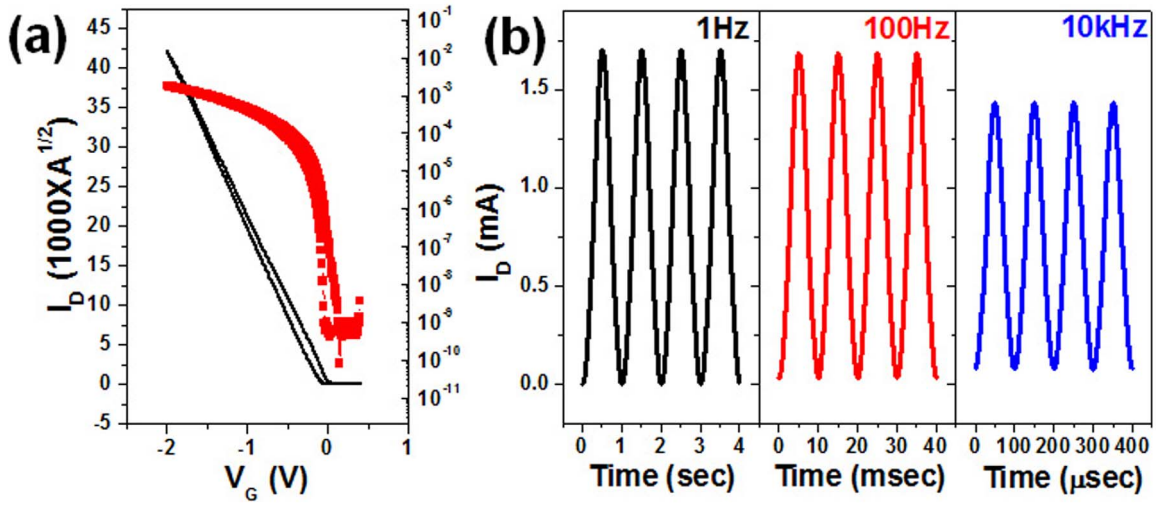

Figure 6 | 2D GIXS patterns for (a) pristine and (b) annealed PDPDBD thin films. (c) and (d) shows corresponding out-of-plane and in-plane profiles, respectively, extracted from 2D GIXS patterns.

In actual application of OFETs, the switching speed against external electrical signal is very important and ideally, the swiching speed is determined by the following relations[50].

$$f = \frac{E\mu}{L} \tag{2}$$

where f is the switching frequency, E is the applied electric field, μ is the field effect mobilty and L is the channel length of targeted OFET. From the equation, we can see that to achieve the maximum frequency under the given device geometry, one has to introduce semiconductors with high mobility. Furthermore, it is known that the electrical hysteresis also introduces energy dissipation and therefore slow down the switching behavior of OFET[51]. Considering the high field effect mobilty and electrical reliability of PDPDBD, we measured the time response of the OFET channel current as a function of variouos frequencies of gate bias pulse. Here, to use commercial funcion generator which has low voltage limit as a source of gate bias pulse, we fabricated low-voltage OFET by using ZrO_x as a dielectric layer. Figure 6 (a) shows that PDPDBD has near-ideal transfer characteristics under low voltage operating condition. The calculated field effect mobility obtained at saturation regime was 1 ~ 2 $cm^2V^{-1}s^{-1}$, consistent with our previous results. Actually, the success of PDPDBD in low voltage operation is very important because commercial transistor-transistor logic (TTL) signal protocol defines V_D = 2–5 V. The drain-source current of targeted transistor shown in Figure 5 with mobilty of 1.4 cm^2/Vs was modulated by applying sinusoidal voltage signal (from 0 to 2 V) between source and gate electrodes. As shown in Figure 6 (b), under the 100 Hz of gate bias pulse, the PDPDBD OFET generated almost identical signal output compared with that under 1 Hz and only slight decrease of signal output is observed under 10 kHz of gate bias pulse. The 3 dB frequency cut-offs of switching frequency was measured to be ~20 kHz, which is very close to the ideal f value obtanined from the carrier transit time, 28 kHz. We suggest that the high mobilty and hysteresis free nature of PDPDBD OFET enabled FET switching speed to approach its theoretical maximum value. Further device optimization such as decrasing channel length can lead to further enhancement of swiching speed.

In order to gain a deeper understanding about the high OFET performance and the improved mobility effect when incorporating DTBDT into the polmer, we investigated the microstructure of the PDPDBD films, prepared under the same conditions used for device fabrication, using 2D grazing-incidence wide-angle X-ray scattering (GIXS) and atomic-force-microscopy (AFM) measurements. Figure 7(a) and (b) display GIXS patterns of PDPDBD without and with thermal annealing at 200°C, respectively. Out-of-plane and in-plane plots extracted from GIXS patterns are also shown in Figure 7(c) and (d), respectively. It is observed that PDPDBD has a crystalline nature with the first out-of-plane diffraction (100) peak at q_z = 0.3 $Å^{-1}$, corresponding to a d-spacing of 21.3 Å. The other two diffraction peaks are attributed to the (200) and (300) diffraction patterns. The broad π-π stacking peak (at q_z = 1.49 $Å^{-1}$) corresponds to a spacing of 4.2 Å. Interestingly, the in-plane diffraction patterns are overall quite similar to the out-of-plane patterns, except that the (l00) peaks are suppressed and the π-stacking peaks are more pronounced in the in-plane diffraction pattern. Furthermore, the diffuse ring centered at the origin has a radius near the π-stacking distance, indicating that a significant portion of the film is disordered. These results imply that PDPDBD does not have either preferentially long-range ordered edge-on or face-on structure, but instead consists of rather disordered small polymer crystalline domains. Although Bragg diffraction peaks become more distinct as a result of thermal annealing, the overall aspects remain similar, in good agreement with our OFET data. Morphological analysis was further conducted using AFM. As shown in Figure S7 (Supplementary Information), both the PDPDBD films without and with thermal annealing show small crystalline domains with an average size of ~100 nm. The only change induced by thermal annealing is an increase in the film roughness. These results imply that PDPDBD does not have the polycrystalline-like microstructure characteristics that are typical for conjugated polymers with high mobilities, but has highly disordered structures with short-range ordered crystalline aggregations. This is an interesting result because DPP-based polymers generally showed high mobilities due to their high crystalline packing structures in a solid state induced by strong intermolecular interactions between the DPP units[6–9]. In comparison, PDPBD showed relatively higher crystallinity in a solid state; the AFM image of the polymer film in Figure S8 revealed well-ordered large crystalline features and the the in-plane scattering profiles extracted from the GIXS shown in Figure S9 and S10 exhibited higher orders of diffraction peaks compared to those of PDPDBD, implying a long rage ordered microstructure in solid state PDPBD. Nonetheless, PDPBD achieved a much lower charge mobility of 0.005 cm^2 $V^{-1}s^{-1}$. Furthermore, the high molecular weight of PDPBD (Mn = 121.9 kg/mol) is known to be advantageous for high charge mobilities because long polymer chains facilitate intermolecular charge transport by increasing interconnectivity between neighbored polymer domains for efficient charge transport[52]. These unusual results are mostly originated from

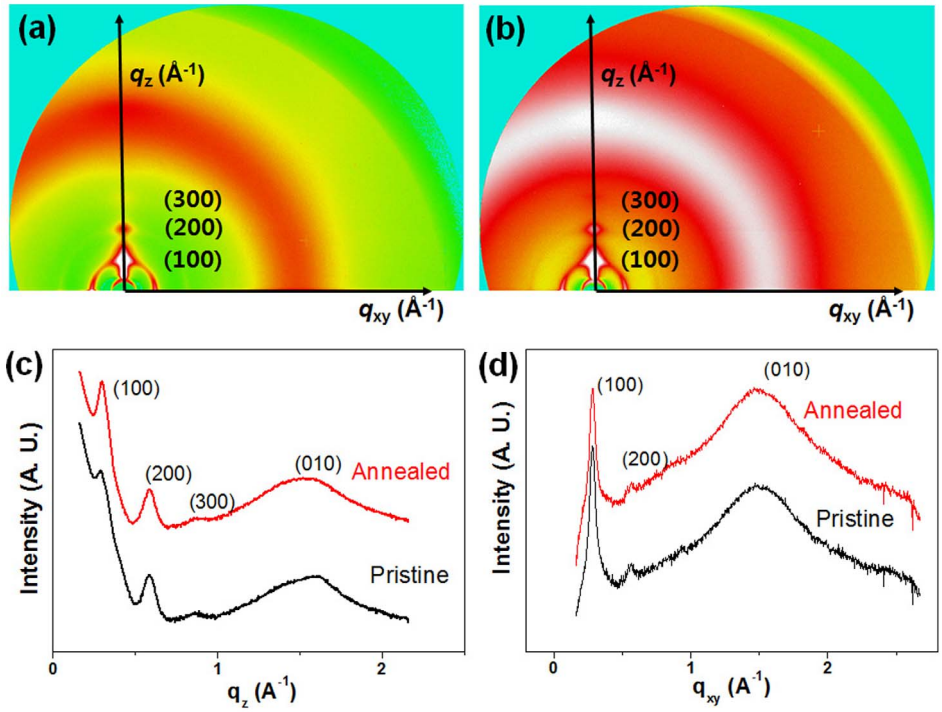

Figure 7 | (a) Transfer characteristics of low voltage transistor using PDPDBD as an active layer and ZrOx as a dielectric layer (b) The result of switching speed measurements. The representative drain current response to a sinusoidal wave signal applied to the gate voltage with various frequencies.

the different molecular structures between the DTBDT and BDT units. When considering charge transport mechanisms of conjugated polymers represented by intra- and intermolecular charge transports, extension of the π-conjugation from BDT to DTBDT affected the polymer's mobility with two different aspects; the enhanced polymer backbone rigidity induced by the large aromatic ring of DTBDT increases the charge mobility due to favorable conduction occuring along the polymer backbone[53] while the decreased crystallinity and lower molecular weight of PDPDBD compared with PDPBD can result in less efficient intermolecular charge transport. Noriega and coworkers reported the important finding that a low crystalline nature in conjugated polymers does not necessarily lead to low charge carrier mobility. From a literature survey of data reported over ten years, it is concluded that the presence of short-range intermolecular aggregations are enough for efficient long-range charge transport[54]. Therefore, it is expected that the intermolecular charge transport occurs efficiently in PDPDBD even at a small aggregate level although the polymer's crystallinity is relatively low. Taken together, we argue that it is highly important to improve intramolecular charge transport in the polymer chain for achiving high mobilities of conjugate polymers. Our results shows that for developing high mobility polymers it is a good design strategy to increase rigidity of the polymer backbone via incorporation of a large aromatic ring. Moreover, such efficient intramolecular charge transport of PDPDBD enabled high charge carrier mobility even without any heat-treatment to improve crystallinity, which is a very beneficial characteristic for application of this polymer in a large area, flexible electronics.

To further demonstrate practical usability of PDPDBD for high performance optoelectronic devices, we tested photodetector peformances of a PDPDBD-based photoconductor. The photoconductor is a gain-generating photodetector device and for achieving a high gain value, charge carrier lifetimes should be long and it is of great importance to employ a high mobility semiconductor[50]. So far organic semiconductors have had less attention as the photoconductor materials compared with inorganic semiconductors mainly due to their low charge carrier mobilities[55–58]. D. Moses and coworkers demonstrated a photoconductor device with a responsivity of 25 A/W and a gain of 82 using an organic semiconductor composite[55]. Similar performances were also reported by using pentacene and poly (*p*-phenylenevinylene) as an active layer[57]. The poor photoconductor performance of organic semiconductors is mainly attributed to either intrinsically low charge carrier mobility or difficulty in generating percolating pathways for efficient charge carrier transport when mixed with sensitizing centers required for charge separation[59].

PDPDBD-based photoconductor was fabricated by using a PDPDBD:C71-butyric acid methyl ester ($PC_{71}BM$) blend film, where $PC_{71}BM$ is a sensitizing center to induce electron trapping and thus extend a hole lifetime in the active layer. The device structure is shown in Figure 8. Morphology of the blend film was optimized with a blend ratio of PDPDBD:$PC_{71}BM$ = 1 : 2 (wt : wt) using a chloroform processing solvent. In the AFM image of the blend film (Figure 8 (a)), bright spots with 100 ~ 300 nm sizes indicate aggregated $PC_{71}BM$. The transistor fabricated using the same condition of the PDPDBD:$PC_{71}BM$ blend film showed hole mobility up to 0.8 $cm^2V^{-1}s^{-1}$, indicating percolated pathways were formed in the blend film. It is notable that the devices processed using other solvents such as chlorobenzene did not result in such high mobilty probably due to forming unoptimized charge transport pathways. Dark and photocurrent – voltage relations were measured under the various light intensities at 760 nm and summarized in Figure 8 (c). Responsivity represented by a ratio of a magnitude of photocurrent and a illuminated light intensity[59] decreased monotonically with increasing the light intensity as shown in a plot of responsivity as a function of illuminated light intensity (Figure 8 (d)). This is a typical feature of the gain-generating photoconductor because excess charge carriers generated by increasing the light intensity result in trap filling and thus less effective trapping mechanism[58,59]. To further study the origin of the photoconductive gain in the device, the transient response was recorded at 760 nm with various light intensities (Figure 8 (e)). The photocurrent decay became slower by decreasing the light intensity, implying the increased carrier lifetime. If the photo-generated electrons in the active layer experience trapping before recombination with holes as assumed in photoconductor,

the rise and decay time in Figure 8(e) can be expressed as $t \sim (1 + \frac{n_t}{n})\tau_n$, where n is the free electron density and n_t is the trapped electron density and τ_n is the recombination time[60]. From the result, it is concluded that decreasing the light intensity increases trapped electron, resulting in a longer carrier lifetime and a higher responsivity. Figure 8 (f) shows gain values derived according to $G = R/(h\nu/q)$ as a function of light intensity[61]. As expected, gain and responsivity have the same light intensity dependence. The obtained gain value is $\sim 10^2$ at 10 μW/cm^2 and increases up to 10^5 at ~20 nW/cm^2. To the best of our knowledge, this value is among the highest values of organic photoconductors[55–62]. Such notable performance of the photoconductor, particularly in terms of photoconductive gain, is attributed to the high charge carrier mobility of PDPDBD. It is believed that the photoconductor performance will be further enhanced via optimization of the sensitizing center and morphology of the active layer.

As a last step, we tested photovoltaic properties of the PDPDBD with a device structure of ITO/PEDOT:PSS (20 nm)/polymer:$PC_{71}BM$ photoactive layer (100 nm)/TiO_2 (10 nm) Al (100 nm). The photoactive layer was fabricated by spin casting of PDPDBD:$PC_{71}BM$ (1 : 2, wt/wt ratio) mixtures dissolved in a chlorobenezene:1,8-diiodooctane cosolvent. The solar cell devices were tested under simulated 100 mW/cm^2 AM1.5G illumination and a current-density and voltage (J-V) curve was obtained as shown in Figure S11. In the preliminary test, a power conversion efficiency (PCE) was achieved up to 4.71% with a short circuit current (J_{sc}) of 9.8 mA/cm^2, an open circuit voltage (V_{oc}) of 0.745 V and a fill factor (FF) of 0.646. With optimization of the device structure and fabrication conditions, the solar cell performance is expected to be further improved and we progress the solar cell study as our ongoing research.

In conclusion, high mobility, hysteresis free, and highly reliable polymer transistors were fabricated from the push-pull type copolymer of DTBDT and DPP. PDPDBD showed a much imporved mobility from PDPBD where DTBDT was replaced by a smaller aromatic ring of BDT although the polymer's crystallinity in the film decreased from PDPBD. PDPDBD achieved charge carrier mobilities up to 2.7 cm^2 V^{-1}s^{-1} under optimized heat-treatment and 1.4 cm^2 V^{-1}s^{-1} without any post-treatment. It is demonstrated that incorporation of large aromatic rings such as DTBDT into the polymer is effective for improving intramolecular charge transport in the polymer chain by making the polymer backbone more rigid. More importantly, the PDPDBD-based OFET showed excellent stability, switching behavior and reliability comparable to a-Si TFTs. Furthermore, due to the high charge carrier mobility, a photocon-

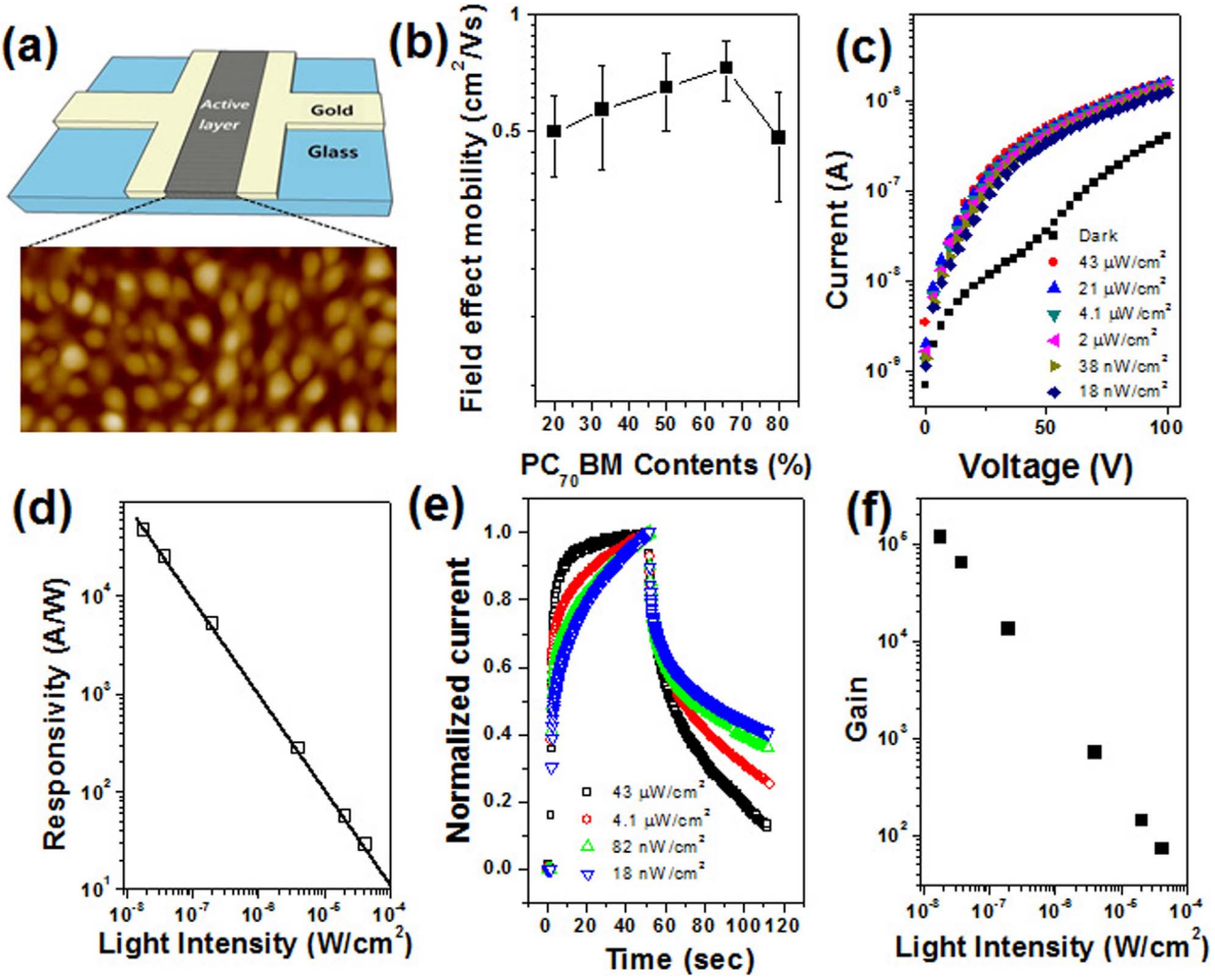

Figure 8 | Summarization of photoconductor measurements. (a) The device schematic combined with AFM image of active layer. The size is 2.5 μm × 5 μm. (b) The field effect mobilty of PDPDBD:$PC_{71}BM$ blend as a function of $PC_{71}BM$ contents. (c) I-V characteristics of photoconductor at dark and various light intensities. (d) The responsivity plots as a function of light intensity. (e) The transient photocurrent under the various light intensities. (f) The photoconductive gain plots as a function of light intensity.

ductor fabricated using PDPDBD achived a high performance with the highest photoconductive gain value ~10^5. Taken together, we demonstrated high potential of PDPDBD as a key material in the quest for low-cost and flexible electronic devices.

1. Arias, A. C., MacKenzie, J. D. & McCulloch, I. Materials and Applications for Large Area Electronics: Solution-Based Approaches. *Chem. Rev.* **110**, 3–24 (2010).
2. Holliday, S., Donaghey, J. E. & McCulloch, I. Advances in Charge Carrier Mobilities of Semiconducting Polymers Used in Organic Transistors. *Chem. Mater.* **26**, 647–663 (2013).
3. Gelinck, G., Heremans, P., Nomoto, K. & Anthopoulos, T. D. Organic Transistors in Optical Displays and Microelectronic Applications. *Adv. Mater.* **22**, 3778–3798 (2010).
4. Di, C.-A., Liu, Y., Gui, Y. & Zhu, D. Interface Engineering: An Effective Approach toward High-Performance Organic Field-Effect Transistors. *Acc. Chem. Res.* **42**,1573–1583 (2009).
5. Zaumseil, J. & Sirringhaus, H. Electron and Ambipolar Transport in Organic Field-Effect Transistors. *Chem. Rev.* **107**, 1296–1323 (2007).
6. Biniek, L., Schroeder, B. C., Nielsen, C. B. & McCulloch, I. Recent advances in high mobility donor–acceptor semiconducting polymers. *J. Mater. Chem.* **22**, 14803–14813(2012).
7. Facchetti, A. π-Conjugated Polymers for Organic Electronics and Photovoltaic Cell Applications. *Chem. Mater.* **23**, 733–758 (2011).
8. Nielsen, C. B., Turbiez, M. & McCulloch, I. Recent Advances in the Development of Semiconducting DPP-Containing Polymers for Transistor Applications. *Adv. Mater.* **25**, 1859–1880 (2012).
9. Shirota, Y. & Kageyama, H. Charge Carrier Transporting Molecular Materials and Their Applications in Devices. *Chem. Rev.* **107**, 953–1010 (2007).
10. Li, J. *et al.* A stable solution-processed polymer semiconductor with record high-mobility for printed transistors. *Sci. Rep.* **2**, 754 (2012).
11. Mei, J., Kim, D. H., Ayzner, A. L., Toney, M. F. & Bao, Z. Siloxane-Terminated Solubilizing Side Chains: Bringing Conjugated Polymer Backbones Closer and Boosting Hole Mobilities in Thin-Film Transistors. *J. Am. Chem. Soc.* **133**, 20130–20133 (2011).
12. Kang, I. *et al.* Effect of Selenophene in a DPP Copolymer Incorporating a Vinyl Group for High-Performance Organic Field-Effect Transistors. *Adv. Mater.* **25**, 524–528 (2013).
13. Chen, H. *et al.* Highly π-Extended Copolymers with Diketopyrrolopyrrole Moieties for High-Performance Field-Effect Transistors. *Adv. Mater.* **24**, 4618–4622 (2012).
14. Lei, T., Dou, J.-H. & Pei, J. Influence of Alkyl Chain Branching Positions on the Hole Mobilities of Polymer Thin-Film Transistors. *Adv. Mater.* **24**, 6457–6461 (2012).
15. Lei, T. *et al.* Ambipolar Polymer Field-Effect Transistors Based on Fluorinated Isoindigo: High Performance and Improved Ambient Stability. *J. Am. Chem. Soc.* **134**, 20025–20028 (2012).
16. Chen, Z. *et al.* High-Performance Ambipolar Diketopyrrolopyrrole-Thieno[3,2-b]thiophene Copolymer Field-Effect Transistors with Balanced Hole and Electron Mobilities. *Adv. Mater.* **24**, 647–652 (2012).
17. Zhong, H. *et al.* Air-Stable and High-Mobility n-Channel Organic Transistors Based on Small-Molecule/Polymer Semiconducting Blends. *Adv. Mater.* **24**, 3205–3211 (2012).
18. Oh, J. H. *et al.* Interplay between Energetic and Kinetic Factors on the Ambient Stability of n-Channel Organic Transistors Based on Perylene Diimide Derivatives. *Chem. Mater.* **21**, 5508–5518 (2009).
19. Jones, B. A., Facchetti, A., Wasielewski, M. R. & Marks, T. J. Tuning Orbital Energetics in Arylene Diimide Semiconductors. Materials Design for Ambient Stability of n-Type Charge Transport. *J. Am. Chem. Soc.* **129**, 15259–15278 (2007).
20. Lei, T. *et al.* High-Performance Air-Stable Organic Field-Effect Transistors: Isoindigo-Based Conjugated Polymers. *J. Am. Chem. Soc.* **133**, 6099–6101 (2011).
21. Okamoto, T. *et al.* Synthesis of regioregular pentacene-containing conjugated polymers. *J. Mater. Chem.* **21**, 7078–7081 (2011).
22. Fong, H. H. *et al.* Tetrathienoacene Copolymers As High Mobility, Soluble Organic Semiconductors. *J. Am. Chem. Soc.* **130**, 13202–13203 (2008).
23. Osaka, I., Abe, T., Shinamura, S., Miyazaki, E. & Takimiya, K. High-Mobility Semiconducting Naphthodithiophene Copolymers. *J. Am. Chem. Soc.* **132**, 5000–5001 (2010).
24. Wu, J.-S., Lin, C. T., Wang, C.-L., Cheng, Y.-J. & Hsu, C.-S. New Angular-Shaped and Isomerically Pure Anthradithiophene with Lateral Aliphatic Side Chains for Conjugated Polymers: Synthesis, Characterization, and Implications for Solution-Prossessed Organic Field-Effect Transistors and Photovoltaics. *Chem. Mater.* **24**, 2391–2399 (2012).
25. Takimiya, K., Shinamura, S., Osaka, I. & Miyazaki, E. Thienoacene-Based Organic Semiconductors. *Adv. Mater.* **23**, 4347–4370 (2011).
26. Xiao, K. *et al.* Highly π-Stacked Organic Semiconductor for Field-Effect Transistors Based on Linearly Condensed Pentathienoacene. *J. Am. Chem. Soc.* **127**, 13281–13286 (2005).
27. He, M. & Zhang, F. Synthesis and Structure of Alkyl-Substituted Fused Thiophenes Containing up to Seven Rings. *J. Org. Chem.* **72**, 442–451 (2007).
28. Balaji, G. & Valiyaveettil, S. Synthesis and Properties of Symmetric and Unsymmetric Dibenzothienopyrroles. *Org. Lett.* **11**, 3358–3361 (2009).
29. Son, H. J., Carsten, B., Jung, I. H. & Yu, L. Overcoming efficiency challenges in organic solar cells: rational development of conjugated polymers. *Energy Environ. Sci.* **5**, 8158–8170 (2012).
30. Hou, J. *et al.* Bandgap and Molecular Energy Level Control of Conjugated Polymer Photovoltaic Materials Based on Benzo[1,2-b:4,5-b′]dithiophene. *Macromolecules* **41**, 6012–6018 (2008).
31. Huo, L. & Hou, J. Benzo[1,2-b:4,5-b′]dithiophene-based conjugated polymers: band gap and energy level control and their application in polymer solar cells. *Polym. Chem.* **2**, 2453–2461 (2011).
32. Son, H. J. *et al.* Synthesis and Photovoltaic Effect in Dithieno[2,3-d:2′,3′-d′]Benzo[1,2-b:4,5-b′]dithiophene-Based Conjugated Polymers. *Adv. Mater.* **25**, 838–843 (2013).
33. Wu, Y. *et al.* PDT-S-T: A New Polymer with Optimized Molecular Conformation for Controlled Aggregation and π–π Stacking and Its Application in Efficient Photovoltaic Devices. *Adv. Mater.* **25**, 3449–3455 (2013).
34. Li, Y., Sonar, P., Murphy, L. & Hong, W. High mobility diketopyrrolopyrrole (DPP)-based organic semiconductor materials for organic thin film transistors and photovoltaics. *Energy Environ. Sci.* **6**, 1684–1710 (2013).
35. Li, Y., Singh, S. P. & Sonar, P. A High Mobility P-Type DPP-Thieno[3,2-b]thiophene Copolymer for Organic Thin-Film Transistors. *Adv. Mater.* **22**, 4862–4866 (2010).
36. Li, Y. *et al.* Annealing-Free High-Mobility Diketopyrrolopyrrole−Quaterthiophene Copolymer for Solution-Processed Organic Thin Film Transistors. *J. Am. Chem. Soc.* **133**, 2198–2204 (2011).
37. Pan, H. *et al.* Low-Temperature, Solution-Processed, High-Mobility Polymer Semiconductors for Thin-Film Transistors. *J. Am. Chem. Soc.* **129**, 4112–4113 (2007).
38. Mei, J., Kim, D. H., Zyzner, A. L., Toney, M. F. & Bao, Z. Siloxane-Terminated Solubilizing Side Chains: Bringing Conjugated Polymer Backbones Closer and Boosting Hole Mobilities in Thin-Film Transistors. *J. Am. Chem. Soc.* **133**, 20130–20133 (2011).
39. Paasch, G., Scheinert, S., Herasimovich, A., Hörselmann, I. & Lindner, T. Characteristics and mechanisms of hysteresis in polymer field-effect transistors. *Phys. Stat. Sol. (a)* **205**, 534–548 (2008).
40. Li, Y. *et al.* Annealing-Free High-Mobility Diketopyrrolopyrrole−Quaterthiophene Copolymer for Solution-Processed Organic Thin Film Transistors. *J. Am. Chem. Soc.* **133**, 2198–2204 (2011).
41. Cheng, H.-L., Lin, W.-Q. & Wu, F.-C. Effects of solvents and vacancies on the electrical hysteresis characteristics in regioregular poly(3-hexylthiophene) organic thin-film transistors. *Appl. Phys. Lett.* **94**, 223302 (2009).
42. Li, Z. *et al.* Alkyl Side Chain Impact on the Charge Transport and Photovoltaic Properties of Benzodithiophene and Diketopyrrolopyrrole-Based Copolymers. *J. Phys. Chem. C.* **115**, 18002–18009 (2011).
43. Kim, S. H., Jang, M., Yang, H. & Park, C. E. Effect of pentacene–dielectric affinity on pentacene thin film growth morphology in organic field-effect transistors. *J. Mater. Chem.* **20**, 5612–5620 (2010).
44. Chung, D. S., Kang, I., Kim, Y.-H. & Kwon, S.-K. Charge transport characteristics of a high-mobility diketopyrrolopyrrole-based polymer. *Phys. Chem. Chem. Phys.* **15**, 14777–14782 (2013).
45. Veres, J., Ogier, S. D., Leeming, S. W., Cupertino, D. C. & Khaffaf, S. M. Low-k Insulators as the Choice of Dielectrics in Organic Field-Effect Transistors. *Adv. Funct. Mater.* **13**, 199–204 (2003).
46. Podzorov, V. *et al.* Intrinsic Charge Transport on the Surface of Organic Semiconductors. *Phys. Rev. Lett.* **93**, 086602 (2004).
47. Bässler, H. Charge Transport in Disordered Organic Photoconductors a Monte Carlo Simulation Study. *Phys. Stat. Sol.* **175**, 15–56 (1993).
48. Mathijssen, S. G. *et al.* Dynamics of Threshold Voltage Shifts in Organic and Amorphous Silicon Field-Effect Transistors. *Adv. Mater.* **19**, 2785–2789 (2007).
49. Deane, S., Wehrspohn, R. & Powell, M. Unification of the time and temperature dependence of dangling-bond-defect creation and removal in amorphous-silicon thin-film transistors. *Phys. Rev. B.* **58**, 12625–12628 (1998).
50. Sze, S. M. & Ng, K. K. *Physics of Semiconductor Devices; 3rd Ed.* [526–527] (J. Wiley & Sons, NewYork, 2007).
51. Chung, D. S. *et al.* Low voltage, hysteresis free, and high mobility transistors from all inorganic colloidal nanocrystals. *Nano Lett.* **12**, 1813–1820 (2012).
52. Zhang, R. *et al.* Nanostructure Dependence of Field-Effect Mobility in Regioregular Poly(3-hexylthiophene) Thin Film Field Effect Transistors. *J. Am. Chem. Soc.* **128**, 3480–3481 (2006).
53. Zhang, X. *et al.* Molecular origin of high field-effect mobility in an indacenodithiophene–benzothiadiazole copolymer. *Nature Commun.* **4**, 2238 (2013).
54. Noriega, R. *et al.* A general relationship between disorder, aggregation and charge transport in conjugated polymers. *Nature Mater.* **12**, 1038–1044 (2013).
55. Hernandez-Sosa, G., Coates, N. E., Valouch, S. & Moses, D. High photoconductive responsivity in solution-processed polycrystalline organic composite films. *Adv. Func. Mater.* **21**, 927–931 (2011).

56. a) Zhou, Y., Wang, L., Wang, J., Pei, J. & Cao, Y. Highly sensitive, air-stable photodetectors based on single organic sub-micrometer ribbons self-assembled through solution processing. *Adv. Mater.* **20**, 3745–3749 (2008).
57. Gao, J. & Hegmann, F. A. Photoconductive gain in pentacene thin films. *Appl. Phys. Lett.* **93**, 223306 (2008).
58. Campbell, I. H. & Crone, B. K. Bulk photoconductive gain in poly(phenylene vinylene) based diodes. *J. Appl. Phys.* **101**, 024502 (2007).
59. Konstantatos, G., Clifford, J., Levina, L. & Sargent, E. H. Sensitive solution-processed visible-wavelength photodetectors. *Nature Photon.* **1**, 531–534 (2007)
60. Bruggemann, R. Analysis of the photoconductive decay from a trapping perspective. *Solid State Commun.* **101**, 199–203 (1997).
61. Soci, C. *et al*. ZnO nanowire UV photodetectors with high internal gain. *Nano Lett.* **7**, 1003–1009 (2007).
62. Chen, H.-Y., Lo, M. K. F., Yang, G., Monbouquette, H. G. & Yang, Y. Nanoparticle-assisted high photoconductive gain in composites of polymer and fullerene. *Nature Nanotechnol.* **3**, 543–547 (2008).

Acknowledgments

This work was supported by the Global Frontier R&D Program on Center for Multiscale Energy System funded by the National Research Foundation under the Ministry of Science, ICT & Future Planning, Korea (2012M3A6A7054856) and Korea Institute of Science and Technology (KIST) for "NAP National Agenda Project Program" of Korea Research Council of Fundamental Science & Technology (KRCF). This work was also supported by the National Research Foundation of Korea (NRF) grant funded by the Korea government (MSIP) (2012047047).

Author contributions

H.J.S. supervised S.P. in polymer design and synthesis. D.S.C. supervised B.T.L. in device fabrication and measurement. B.K. contributed to material design. H.J.S. and D.S.C. directed the overall project and wrote the manuscript.

Additional information

Supplementary information accompanies this paper at http://www.nature.com/scientificreports

Competing financial interests: The authors declare no competing financial interests.

How to cite this article: Park, S., Lim, B.T., Kim, B., Son, H.J. & Chung, D.S. High mobility polymer based on a π-extended benzodithiophene and its application for fast switching transistor and high gain photoconductor. *Sci. Rep.* **4**, 5482; DOI:10.1038/srep05482 (2014).